激光－电弧复合焊接过程中等离子体的耦合行为

陈明华， 李陈宾， 刘黎明
(大连理工大学 辽宁省先进连接技术重点实验室，大连 116024)

摘 要：激光－电弧复合热源可以形成3种焊缝横截面的形貌，根据焊接参数对焊缝横截面形貌的影响建立了激光和电弧等离子体相互作用的物理机制. 通过考察复合焊接过程中电弧等离子体中原子分布状态、电弧辐射光谱信息以及激光“匙孔”的行为对机制进行了验证. 结果表明，激光对电弧等离子体的作用是通过激光形成的“匙孔”及其内部等离子体实现的，在适当参数下，电弧等离子体弧柱会进入激光“匙孔”内部，并与“匙孔”等离子体发生耦合放电，最终形成复合等离子体. 电弧等离子体和“匙孔”等离子体的耦合作用有利于提高热源的能量密度.

关键词：激光－电弧复合热源；匙孔；等离子体；机制
中图分类号：TG 403 **文献标识码**：A **文章编号**：0253－360X(2014)10－0053－04

0 序 言

激光－电弧复合热源将激光、电弧两种物理本质完全不同的热源有机复合在一起，它不但继承了两种热源各自的优点、避免了各自的缺点，同时二者的有机复合也产生了很多新的特征[1]. 近年来，国内外研究者围绕该复合热源焊接技术开展了大量研究工作. 结果表明，相比单一电弧热源和激光热源加工，激光－电弧复合热源具有更强的热穿透能力、更稳定的加工过程以及更高的加工效率[2,3]. 目前，研究的热点主要集中于激光－电弧复合热源加工过程的工艺研究、专用设备研制和接头性能测试与质量评估等工程应用开发层面，而对激光和电弧的相互作用以及复合热源本质特性的研究报道却较少. 已有的研究报道显示，在激光－电弧复合焊接过程中，激光可以诱导和增强电弧等离子体放电，提高电弧燃烧的稳定性，同时电弧的预热作用提高了材料对激光的吸收率；在激光的作用下金属板材的原子会对电弧等离子体的放电状态产生影响[4－6].

焊接过程中，焊缝横截面的形貌特征可以直接反映热源本身的状态. 因此，文中以复合热源形成的焊缝横截面形貌为切入点，通过考察焊接参数对焊缝横截面形貌的影响，建立了激光－电弧复合热源焊接过程中脉冲激光与电弧等离子体相互作用的模型，再通过电弧光谱辐射特性、电弧等离子体和“匙孔”行为等角度的试验对该机制进行验证.

收稿日期：2014－04－12
基金项目：国家科技重大专项资助项目(2012ZX04008031)

1 试验方法

采用脉冲式 Nd:YAG 激光、钨极氩弧(gas tungsten arc，GTA)焊接电源以及控制系统构建激光－电弧复合焊接系统对6 mm厚AZ61镁合金板材实施平板堆焊试验. 试验装置示意图如图1所示.

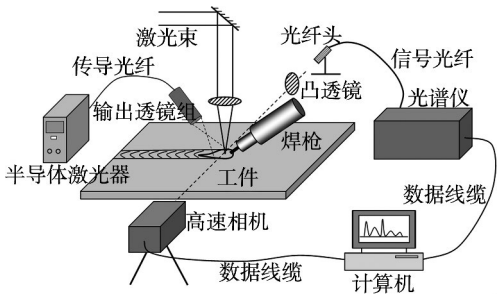

图1 试验装置示意图
Fig. 1 Sketch of experimental device

图1中钨极(含 CeO_2 约2%)直径为3.2 mm，顶角约30°，GTA焊枪与激光束在焊接方向上呈45°夹角，采用电弧在前的焊接方式，激光束轴线与GTA钨极尖端距离(D_{la})在试验中可变，焊接速度800 mm/min. 采用纯度为99.99%的氩气作为焊接保护气体，其流速为10 L/min. 采用高速摄像机(采样率3 000帧/s)对电弧等离子体侧面形态进行观测，根据电弧等离子体的光谱辐射特征，分别采用516 nm和808 nm的带通滤光片对电弧等离子体中的Ar原子和Mg原子行为进行检测. 同时，在半导体激光照明光源(808 nm波长)的辅助下，对焊接电弧和熔池

状态进行直接的、高时间分辨率的观测. 采用直读光谱仪对焊接等离子体光辐射状态进行采集和分析. 焊后对焊缝的横、纵截面进行打磨、抛光,并用盐酸酒精溶液(5% HCl + 95% C_2H_5OH)腐蚀,观察热源的作用效果.

2 试验结果及分析

2.1 试验结果

激光 - 电弧复合热源的焊缝横截面通常会出现如图 2a ~ 图 2c 所示的 3 种形貌,文中分别将其抽象后所得示意图如图 2d ~ 图 2f 所示,分别定义为 A,B,C 型,其反映了不同复合状态的热源作用效果. 图 2a 表明激光和电弧近似独立地作用于材料,二者的协同作用较小; 图 2b 和图 2c 体现了激光和电弧之间的耦合作用.

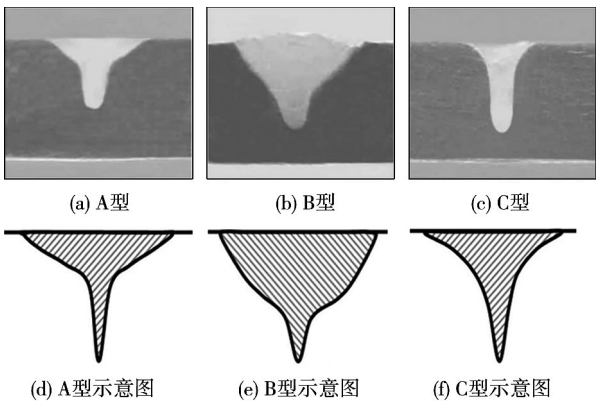

图 2 复合热源形成的焊缝横断面的形貌

Fig. 2 Cross-sections of laser-arc hybrid welding seam

图 3 为复合热源焊缝横截面形貌与焊接参数(焊接电流、激光功率、D_{la})的关系. 由图 3 可见,激光功率、D_{la} 和电弧电流共同影响焊缝横截面的形貌. 当激光功率为 450 W 时,焊接电流为 40 A 且 D_{la} = 1 mm 时,出现 C 型焊缝横截面形状,此时,继续增大 D_{la} 会先后出现 B 型和 A 型形状; 而大焊接电流情况与小电弧电流情况不同,如 160 A 时,在 D_{la} 较小时焊缝截面呈现 A 型,随着 D_{la} 增大出现 B 型截面,而在试验参数范围内未出现 C 型截面. 当采用 300 W 功率的激光与电弧复合时,出现 C 型和 B 型截面的参数范围在一定程度上缩小,而出现 A 型截面的参数范围扩大. 对比图 3a 和图 3b 发现,C 型焊缝截面只在焊接电流相对较小的区域内出现,在焊接电流为 160 A 时,很难出现 C 型形状; 同时,大的激光功率有利于扩大出现 B 型和 C 型形貌的参数范围.

2.2 机制的提出

根据试验结果建立激光 - 电弧相互作用的机制

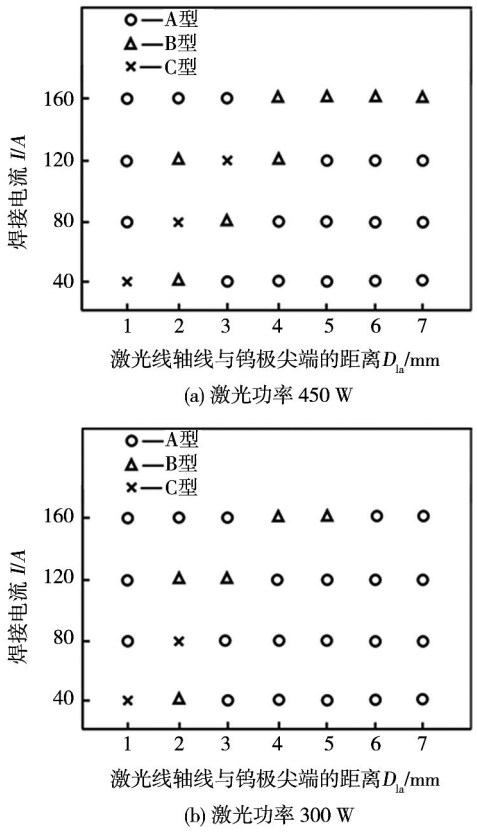

图 3 焊接参数对焊缝横截面形貌的影响

Fig. 3 Influence of welding parameters on morphology of weld cross-section

如下: 当激光在镁合金板材表面形成“匙孔”时,“匙孔”内产生高温、高密度的镁等离子体. “匙孔”的高温环境和大量的 Mg 离子和电子为电弧等离子体提供优良的放电环境,电弧等离子体根部位置会移动至“匙孔”处形成复合放电,如图 4 所示.

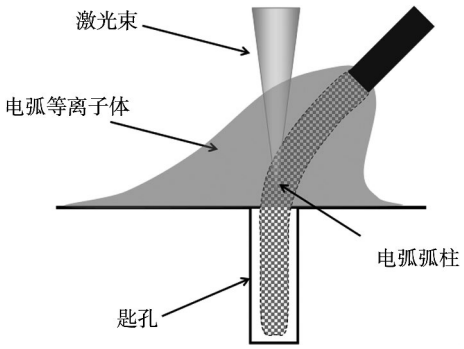

图 4 电弧等离子体与“匙孔”等离子体的复合放电

Fig. 4 Discharge of arc plasma and keyhole plasma

2.3 机制的验证

2.3.1 电弧等离子体状态分析

根据上述机制,复合放电状态时,Mg 离子从“匙孔”进入电弧导电通道将导致复合电弧等离子体中

Mg 原子辐射强度的大幅提高. 因此，采用光谱仪对电弧等离子体导电通道中 Mg 原子和 Mg 离子的特征发光谱线进行采集，并对比分析激光脉冲作用前后其辐射强度，试验结果如图 5 所示. 由图 5 可以看出，在激光脉冲作用时电弧等离子体中 Mg 原子辐射谱线(Mg Ⅰ线) 急剧升高，表明大量的 Mg 原子进入电弧中. 由于在电弧等离子体外围存在从钨极到板材的高速等离子流，这导致电弧外围的 Mg 原子很难进入内部导电通道[7]. 因此复合电弧导电通道内的 Mg 原子主要来自“匙孔”.

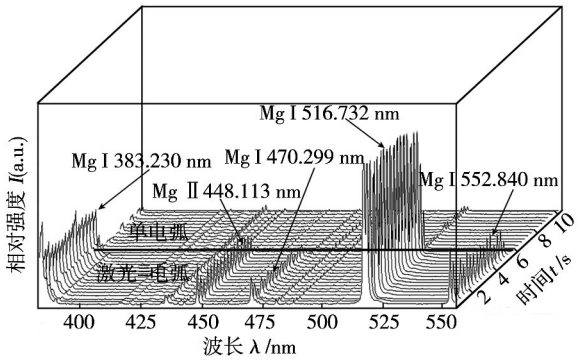

图 5　激光脉冲作用前后 Mg 元素特征谱线强度对比

Fig. 5　Mg element emission intensity variation after laser pulse action

由 2.2 节中建立的机制可知，复合放电等离子体中粒子的分布应该具有区域集中的特点. 由于 Mg 原子的第一电离能(7.6 eV) 低于 Ar 原子(15.7 eV) ，因此当“匙孔”中 Mg 原子进入电弧导电通道时，会大量地取代 Ar 原子进行电离导电，即形成如图 6 所示的 Ar 原子分布空间被压缩至钨电极附近的状态.

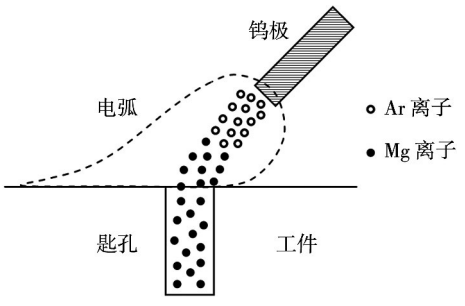

图 6　复合电弧中粒子分布状态示意图

Fig. 6　Particle distributions in arc plasma

试验中，对复合放电电弧中 Ar 原子的分布状态进行实际观测，结果如图 7 所示. 由图 7 可以看出，无激光脉冲作用时 Ar 原子分布于整个电弧弧柱区域; 而在激光脉冲作用时(1.0 ~ 3.0 ms) ，Ar 原子分布区域收缩至钨极附近. 同时，靠近熔池的弧柱区几乎观测不到 Ar 原子的光辐射，这是由于在激光脉冲作用时，电弧等离子体与“匙孔”等离子体发生复合放电，“匙孔”等离子体中大量 Mg 离子在电弧电场作用下迁移至靠近熔池的电弧弧柱区，由于带通滤光片的波长选择作用而不能被观测到. 同时，图 7 中 5.0 ms 时的 Ar 原子分布表明当激光脉冲结束后，电弧的弧柱仍趋向于向“匙孔”内部伸展. 由于此时“匙孔”中镁原子(离子) 供给不足，导致 Ar 原子逐渐恢复电弧导电的主导地位. 因此，从电弧等离子体中粒子分布的角度证明了机制的存在性.

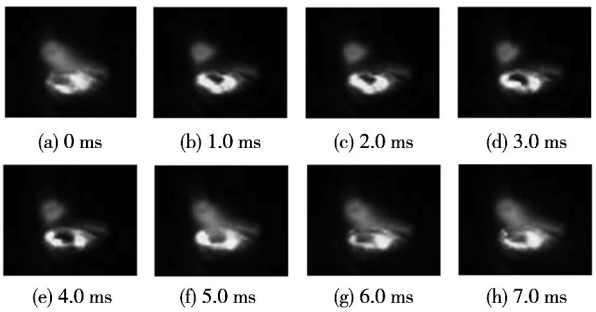

图 7　激光脉冲作用下不同时刻 Ar 原子分布状态

Fig. 7　Ar atom distribution in different time during laser pulse action

2.3.2　激光“匙孔”行为的直接观测

根据 2.2 中建立的机制，在激光脉冲作用时，电弧等离子体弧柱区延伸入激光匙孔内部与“匙孔”等离子体复合，因此电弧弧柱对“匙孔”内壁的压力将阻碍“匙孔”的坍塌. 为了对此进行验证，采用辅助单色光照明、滤光和衰减等一系列光学调制手段，并结合高速摄影的方法对复合焊接过程中电弧形态和“匙孔”状态进行了同步观测，结果如图 8 所示.

从图 8 可见，激光脉冲作用期间(1 ~ 4 ms) ，“匙孔”逐渐形成，激光脉冲作用结束后“匙孔”未立即闭合，“匙孔”开口存在 10 ms 左右. 这是由于当电弧等离子体与“匙孔”等离子体复合后，电弧弧柱深入“匙孔”内部. 此时，在电弧等离子体对“匙孔”内壁的持续压力作用下，“匙孔”的坍塌和闭合过程发生延迟. 同时，该延迟效果会导致“匙孔”内部 Mg 离子注入复合电弧等离子体时间的变长.

图 9 为采用 516 nm 滤光片对电弧等离子体中 Mg 原子整体行为的观测结果. 结果表明，在激光脉冲作用(0 ~ 3 ms) 结束后，电弧等离子体中过量的 Mg 原子并未立刻消散，而是经过一段时间(4 ~ 7 ms) 后才能回复至激光脉冲作用之前的状态，这是

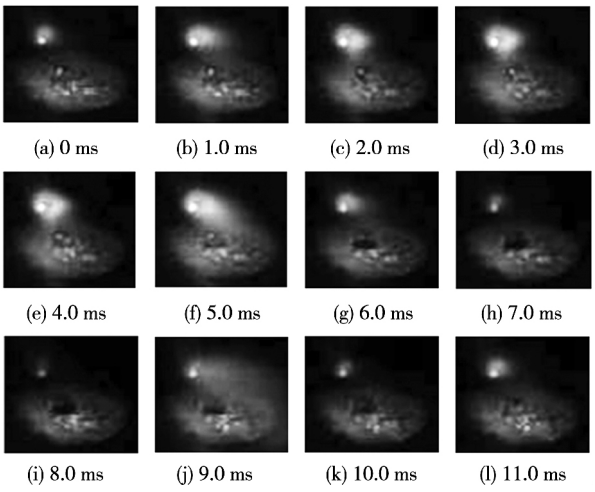

图 8 复合焊接过程中不同时刻“匙孔”行为

Fig. 8 Keyhole behavior in different time during hybrid welding process

“匙孔”等离子体中 Mg 离子向电弧弧柱的持续迁移造成的. 因此对复合焊接过程中“匙孔”行为的观测结果可以对提出机制进行证明.

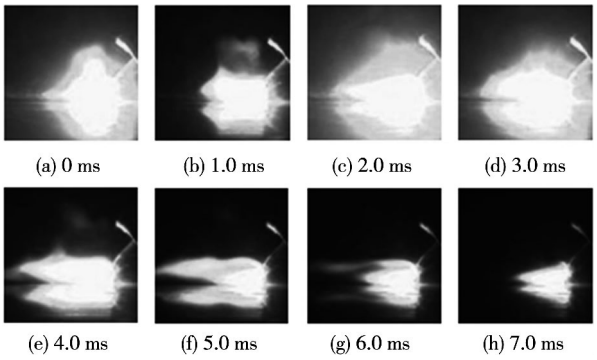

图 9 激光脉冲作用之后电弧中 Mg 原子状态的延迟恢复

Fig. 9 Recovery delay of Mg atom state in arc plasma after laser pulse action

综上所述,在 2.2 节中提出的机制是合理的,根据该机制可以对 2.1 节的试验结果进行较好的解释. 当电弧电流较小时,电弧弧柱直径较小,“匙孔”的尺度和其内等离子体可以承载电弧放电,电弧放电位置稳定,复合热源能量密度和热穿透能力提高,因此焊缝的横截面多呈如图 2c 所示的形貌; 而当电弧电流较大时,“匙孔”等离子体电导率难以完全满足电弧放电需求,电弧与“匙孔”放电的同时也与附近熔池表面放电,因此,会出现图 2b 所示的横截面形貌; 当电弧等离子体和“匙孔”等离子未发生耦合放电时,激光和电弧之间的相互增强作用较弱,出现图 2a 所示的焊缝横截面形貌. 总的来说,焊缝横截面的形貌可以反映激光和电弧耦合之后复合热源整体的能量密度分布特性.

3 结 论

(1) 在激光 - 电弧复合焊接过程中,激光和电弧等离子体的相互作用是以激光在材料表面形成的“匙孔”及其内部等离子体为媒介实现的.

(2) 电弧等离子体弧柱会进入激光“匙孔”,并与“匙孔”等离子体发生耦合作用,形成复合放电等离子体. 电弧等离子体和“匙孔”等离子体的耦合作用有利于提高复合热源的能量密度和热穿透能力.

参考文献:

[1] Steen W M. Arc augmented laser processing of materials [J]. Journal of Application Physics, 1980, 51(11): 5636 - 5641.

[2] 王旭友, 滕 彬, 雷 振, 等. JFE980S 高强钢激光 - 电弧复合热源热模拟试验分析 [J]. 焊接学报, 2010, 31(11): 25 - 28.
Wang Xuyou, Teng Bin, Lei Zhen, *et al*. Analysis on laser-arc hybrid welded joint of high strength stell JFE980S by thermal simulation test [J]. Transactions of the China Welding Instituion, 2010, 31(11): 25 - 28.

[3] 庄忠良, 宋 刚, 祝美丽, 等. 激光 - MIG 复合热源铝合金层间堆积快速成形 [J]. 焊接学报, 2013, 34(5): 71 - 74.
Zhuang Zhongliang, Song Gang, Zhu Meili, *et al*. Rapid prototyping of aluminum alloy with vertical deposition by laser-arc hybrid heat source [J]. Transactions of the China Welding Instituion, 2013, 34(5): 71 - 74.

[4] 吴圣川, 周鑫淼, 张卫华, 等. 激光 - 电弧复合焊接 7075-T6 铝合金裂纹扩展分析 [J]. 焊接学报, 2013, 34(2): 5 - 8.
Wu Shengchuan, Zhou Xinmiao, Zhang Weihua, *et al*. Fatigue life prediction of laser-MIG hybrid welded 7075-T6 Al alloy joint [J]. Transactions of the China Welding Instituion, 2013, 34(2): 5 - 8.

[5] Xu G X, Wu C, Qin G S, *et al*. Effect of laser-wire distance on temperature distribution in laser + GMAW-P hybrid welding [J]. China Welding, 2011, 20(1): 22 - 27.

[6] Gu X Y, Li H, Yang L J, *et al*. Influence of laser on arcs in alternate arcing during laser-twin-arc hybrid welding process [J]. China Welding, 2012, 21(3): 55 - 60.

[7] Shi Y X, Peng R H. Welding arc phenomenon [M]. Beijing: China Machine Press, 1985.

作者简介: 陈明华,男,1983 年出生,博士研究生. 主要从事激光 - 电弧复合热源焊接技术和机制研究. 发表论文 11 篇. Email: cmh@mail.dlut.edu.cn

通讯作者: 刘黎明,男,教授. Email: liulm@dlut.edu.cn

Effect of pulse frequency on microstructure and properties of Ti-6Al-4V joints under condition of low duty cycle

YANG Zhou[1], QI Bojin[1], CONG Baoqiang[1], YANG Mingxuan[1], GAO Mingjian[1,2] (1. School of Mechanical Engineering and Automation, Beihang University, Beijing 100191, China; 2. China Petroleum Material Corporation, Beijing 100029, China). pp 37 -40

Abstract: The microstructure and mechanical properties of Ti-6Al-4V titanium alloys joints was studied, which obtained by ultra high frequency pulse gas tungsten arc welding (UHFP-GTAW) process on the condition with 20% duty cycle. The degree of grain refinement was characterized by the average grain size in fusion zone (FZ). The characteristic of UHFP-GTAW joints microstructure was investigated, and the effect of pulsed current frequency on grain refinement and mechanical properties was also analyzed under condition of low duty cycle. The results showd that in contrast with conventional GTAW (C-GTAW) process, the microstructure of the FZ remained mainly basketweave, and most of α′ phase of the HAZ presented as short-acicular for UHFP-GTAW process. The grains were refined significantly and the average grain size in FZ was decreased by 32% at most. Elongation and reduction of area were increased by 140% and 275%, respectively. Morerover, the ductility of the joints was improved strikingly. In comparision with the 16.7% decline of average grain size in FZ on 50% duty cycle, grains were refined further, and elongation and reduction of area were respectively enhanced by 22% and 33% as the duty cycle was reduced to 20%.

Key words: titanium alloy; ultra high frequency pulsed current; GTAW; basketweave microstructure; mechanical properties

Arc morphology and weld pool flowing in A-MAG welding process

LU Hao[1], XING Jingwei[2], XING Liwei[1], LIANG Zhimin[3] (1. CSR Qingdao Sifang Co. Ltd., Technique Headquarters, Qingdao 266111, China; 2. Shenyang Aerospace University, Faculty of Aerospace Engineering, Shenyang 110136, China; 3. Faculty of Material Science and Engineering, Hebei University of Science & Technology, Shijiazhuang 050000, China). pp 41 -44

Abstract: A-MAG welding process was proposed, by which welded joints of high quality can be obtained. Arc morphology and weld pool flowing of A-MAG welding are observed and analyzed. In which the flow of molten pool was studied by using the tungsten particle tracer method. The test results show that the A-MAG welding arc is shrinking. The weld pool is more concentrated, the flow direction of liquid metal in the molten pool is from the periphery to the centre and the flow is more orderly. The change of the fluid flow in the molten pool is main factor of increased penetration.

Key words: activating flux MAG welding; weld pool flowing; arc morphology

Welding characteristics of aluminum alloy with pre-melting liquid filler

PENG Jin[1], LI Liqun[1], LIN Shangyang[1,2], DENG Zhou[1] (1. State Key Laboratory of Advanced Welding and Joining, Harbin Institute of Technology, Harbin 150001, China; 2. Harbin Welding Institute, Harbin 150080, China). pp 45 -48

Abstract: The influence of welding parameters on filling behavor of aluminum alloy joining with pre-melting liquid filler was researched by using high-speed camera and experimental tests. The quality of welded joints was analyzed as well. The results show that two filling modes, filler wire with partial melting state and full melting state, can be founded in laser welding with pre-melting liquid filler. Liquid filler flows along the wire to molten pool when the filler metal is in partial melting state with small welding current. While in the full melting state with the large welding current, the liquid filler can flow stably into the molten pool with the help of capillary action. With the increase of welding speed, the distance between the keyhole and the weld pool edge became short. The distance between laser beam and filler should be controlled at -0.5-2.0 mm for stable feed of liquid filler to the molten pool. The porosity rate of joints welded with pre-melting liquid filler decreased obviously compared to laser welding with no-melting filler wire.

Key words: laser welding; welding with pre-melting liquid filler; high-speed camera; aluminum alloy

Effect of slagging flux on Fe-Al intermetallic coatings synthesized by laser cladding

WANG Jing, ZOU Yong, JIA Shengkai, YU Lei (Key Lab of Liquid Structure and Heredity of Materials of Ministry of Education, Shandong University, Jinan 250061, China). pp 49 -52

Abstract: The iron-aluminide intermetallic coatings were in-situ synthesized on Q235 steel by laser cladding. The cladding powders were mixed iron and aluminum powders with or without slagging flux. The effects of slagging flux on the microstructure and properties of the cladding coatings were studied. The results indicate that adding slagging flux into the cladding powders not only refines the grains of the cladding layers, but also has a significant influence on the properties of the iron-aluminide coatings. The XRD results show that the main phases of the iron-aluminide coatings both are FeAl with B2 phase structure and Fe_3Al with DO3 phase structure, but the ratio of Fe_3Al increases as slagging flux was added. In addition, the iron-aluminide cladding layers with slagging flux shows higher microhardness, better oxidation resistance and better corrosion resistance than those free of slagging flux.

Key words: laser cladding; iron-aluminide; slagging flux; oxidation resistance; corrosion resistance

Coupling behavior of plasmas during laser-arc hybrid welding process

CHEN Minghua, LI Chenbin, LIU Liming (Key Laboratory of Liaoning Advanced Welding and Joining Technology, Dalian University of Technology, Dalian 116024, China). pp 53 -56

Abstract: Three kinds of welding seam cross-sectional pattern can be found in laser-arc hybrid welding of magnesium alloy. According to the influence of welding parameters on the patterns, the interactive mechanism was proposed. By investigating the atom distributions in the arc plasma, the plasma spectral information and laser keyhole behavior, the mechanism was verified as well. Results show that the effect of laser on arc plasma is realized by both the laser keyhole and the plasma in the keyhole. At certain proper parameters, the arc plasma collumn can extend into the lase keyhole, and discharge with the keyhole plasma. A hybrid plasma can be formed finally. The coupling of arc plasma and keyhole plasma in this style can improve the energy density of the heat source.

Key words: laser-arc hybrid heat source; keyhole; plasma; mechanism